

# Evaluation of Pathological Manifestations of Disease in Mucopolysaccharidosis VII Mice after Neonatal Hepatic Gene Therapy

Lingfei Xu,<sup>1,2</sup> Robert L. Mango,<sup>1</sup> Mark S. Sands,<sup>1,3</sup> Mark E. Haskins,<sup>4</sup>  
N. Matthew Ellinwood,<sup>4</sup> and Katherine Parker Ponder<sup>1,2,\*</sup>

<sup>1</sup>Department of Internal Medicine, <sup>2</sup>Department of Biochemistry and Molecular Biophysics, and <sup>3</sup>Department of Genetics, Washington University School of Medicine, St. Louis, Missouri 63110

<sup>4</sup>Department of Pathobiology, University of Pennsylvania School of Veterinary Medicine, Philadelphia, Pennsylvania 19104

\*To whom correspondence and reprint requests should be addressed at the Department of Internal Medicine, Washington University, Box 8125, 660 S. Euclid Avenue, St. Louis, MO 63110. Fax: (314) 362-8813. E-mail: kponder@im.wustl.edu.

Mucopolysaccharidosis VII (MPS VII) is a lysosomal storage disease caused by  $\beta$ -glucuronidase (GUSB) deficiency. Intravenous injection of a retroviral vector expressing canine GUSB into neonatal MPS VII mice resulted in transduction of 6 to 35% of hepatocytes, which secreted GUSB into blood. Serum GUSB activity was stable for 6 months at 600 (low expression) to 10,000 (high expression) U/ml, and enzyme was modified appropriately with mannose 6-phosphate. The average serum GUSB activity (3531 U/ml) is the highest long-term expression reported for MPS VII mice after gene therapy. Secreted enzyme was taken up by other tissues, as the average enzyme activity was >13% of normal in somatic organs and 2% of normal in brain. Low expression markedly reduced histopathological evidence of lysosomal storage in liver, spleen, kidney, small intestine, neurons, and glial cells. High expression appeared to be more effective than low expression at reducing lysosomal storage in aorta, heart valves, thymus, bronchial epithelium, cornea, and retinal pigmented epithelium. Future experiments will determine if greater pathological improvements will consistently be observed in retrovirus-treated MPS VII mice with higher serum GUSB activity relative to animals with lower activity and if these result in clinical benefits.

**Key Words:** gene therapy, retroviral vector,  $\beta$ -glucuronidase, mucopolysaccharidosis, lysosomal storage disease, glycosaminoglycans, neonatal, liver

## INTRODUCTION

Lysosomal storage diseases (LSD) have an overall incidence of ~1:7700 live births [1] and are caused by deficient activity in enzymes that degrade various intracellular compounds. The mucopolysaccharidoses (MPS) are a subset of LSD that involve the inability to degrade glycosaminoglycans (GAGs). MPS VII, which is caused by deficient  $\beta$ -glucuronidase (GUSB; EC 3.2.1.31) activity, results in growth retardation, poor mobility, dysostosis multiplex, facial dysmorphism, hepatosplenomegaly, corneal clouding, cardiac valvular abnormalities, and mental retardation in humans [1–4]. Although it is one of the rarest of the MPS syndromes, the availability of MPS VII mice [5], dogs [6], and cats [7] has made it an important model system for testing gene therapy approaches for this class of disorders. The MPS VII mouse has a single base pair deletion, resulting in a frameshift at codon 490 of the

648-amino-acid precursor protein, and hence does not express the C-terminal 159 amino acids [8].

GUSB is modified posttranslationally within the Golgi to contain mannose 6-phosphate (M6P), which allows most of the GUSB produced by a cell to be transported directly to the lysosome via the M6P receptor (M6PR) [9]. However, some mannose-6-phosphorylated enzyme is secreted and can be taken up by adjacent cells since the M6PR is also present on the plasma membrane of most cells. This pathway allows cells to take up enzyme from blood after intravenous (iv) injection, as occurs during enzyme replacement therapy (ERT), which is therapeutic for MPS VII mice [10–14]. The M6P is necessary for efficient uptake by most organs, although cells of the reticuloendothelial system can take up enzyme without M6P via other mechanisms [15].

The rationale for using hepatic gene therapy to treat

MPS VII is that transduced liver cells will secrete enzyme with M6P into blood, and enzyme that is taken up by other organs will prevent or ameliorate disease manifestations [reviewed in 16]. Transduction of hepatocytes with retroviral vectors (RV) [17,18], adenovirus-associated virus (AAV) vectors [19–22], or adenoviral vectors [23–27] resulted in the appearance of GUSB in the blood and reduction in lysosomal storage in MPS VII mice. In addition, we recently reported that neonatal hepatic gene therapy with an RV resulted in stable secretion of GUSB with M6P into the blood in MPS VII dogs [28] and prevented the development of many of the clinical manifestations [29]. This work was performed to determine the effect of different serum GUSB levels upon pathological abnormalities in MPS VII mice. These results will be followed by a future study to determine if these pathological differences are clinically significant. Together, these data may lead to predictions regarding the serum GUSB activity necessary to prevent different manifestations of disease in MPS VII.

## RESULTS

### Neonatal Delivery of hAAT-cGUSB-WPRE to MPS VII Mice

RV-treated mice were MPS VII mice that were injected iv with  $1 \times 10^{10}$  red-forming units (rfu)/kg of hAAT-cGUSB-WPRE at 3 days after birth. This is an amphotropic Moloney murine leukemia virus (MLV)-based RV in which the liver-specific human  $\alpha_1$ -anti-trypsin (hAAT) promoter and the woodchuck hepatitis virus posttranscriptional regulatory element (WPRE) are present upstream and downstream, respectively, of the canine GUSB (cGUSB) cDNA [28]. This represents a multiplicity of infection of 1.2 rfu per hepatocyte, based upon the assumptions that the liver is 5% of the body weight, there are  $1.7 \times 10^8$  hepatocytes per gram of liver [30], and all RV particles reach the liver after an iv injection. Animals were sacrificed at 6 months after treatment to allow pathology in RV-treated animals to be compared with that of age-matched untreated MPS VII controls, which have a shortened life span [5].

### Serum GUSB Activity

Hepatocytes of RV-treated mice secreted GUSB into blood, as serum GUSB levels were  $3531 \pm 1258$  [standard error of the mean (SEM)] U/ml (127-fold that of homozygous normal mice) for 6 months after gene transfer (Fig. 1A). Animals referred to as having low serum GUSB activity include D13 (average of 581 U/ml GUSB activity in serum over the 6-month period of analysis) and D14 (947 U/ml). Animals with medium serum GUSB activity include D11 (1844 U/ml), D12 (2733 U/ml), and D10 (2890 U/ml). Animals with high GUSB activity include D9 (5649 U/ml) and D8 (10,070 U/ml). In normal mice,  $22.9 \pm 1.6\%$  (SEM) of the serum GUSB contained M6P. In RV-treated mice,  $34.2 \pm 2.9\%$  of the serum GUSB contained M6P (not

significant vs values in normal mice). Serum GUSB was mannose 6-phosphorylated at a normal percentage even for RV-treated mice with the highest serum GUSB activity (Fig. 1B).

### Analysis of Transduction Efficiency in Organs

We analyzed DNA isolated from organs at 6 months after treatment using real-time PCR for the WPRE sequence of the RV and normalized it to the  $\beta$ -actin sequence of the mouse genome. The average for the seven RV-treated mice was  $0.40 \pm 0.13$  (SEM) copies of the RV per cell in the liver. RV-treated mice with higher serum GUSB activity had more copies of RV DNA per cell than did those with lower GUSB activity (Fig. 1C). We determined the RV DNA copy number in other organs for the three RV-treated mice with the highest serum GUSB activity. The RV DNA sequences were undetectable ( $<0.002$  copies per cell) in large intestine, brain, and gonads and were 14% or less of the value in liver for other organs (Fig. 1D). Since the RV contains the LTR in addition to the hAAT promoter, the low levels of DNA present in some organs could result in expression. Therefore we performed real-time RT-PCR on RNA isolated from liver and other organs (Fig. 1D). This demonstrated that all organs except for muscle contained very low amounts of RV RNA, which varied from 0.1 to 0.6% of the value in liver. These data suggest that the liver was the major organ that expressed cGUSB.

We determined the percentage of hepatocytes that expressed the cGUSB cDNA from the RV by histochemical staining for GUSB activity. Hepatocytes from untreated MPS VII mice have no detectable GUSB activity after an overnight stain (Fig. 2A). Hepatocytes from normal animals have low levels of activity (Fig. 2B), although all cells are positive after a longer stain (not shown). At 6 months after injection of RV, 6% of the hepatocytes had very high levels of GUSB activity for an animal with low serum GUSB activity (Fig. 2C), which is likely due to transduction. These cells were present in large clusters, which probably represent clonal expansion of transduced hepatocytes during postnatal growth. After a longer GUSB stain, numerous bright red clusters were still identified at low power (Fig. 2D). In addition, the entire liver had faint activity, which likely represents uptake of enzyme from blood or adjacent transduced cells. The highest percentage of hepatocytes with high GUSB activity was 35% for D8, and the average for all RV-treated mice was  $19 \pm 3.8\%$ . The fraction of hepatocytes that expressed the cGUSB cDNA of the RV at high levels was approximately half the number of copies per cell in individual animals (Fig. 1C).

### GUSB and $\beta$ -Hexosaminidase Activity in Organs

We determined GUSB activity in liver homogenates at 6 months after treatment. Prior to sacrifice, mice were perfused with saline to reduce the possibility that some ac-

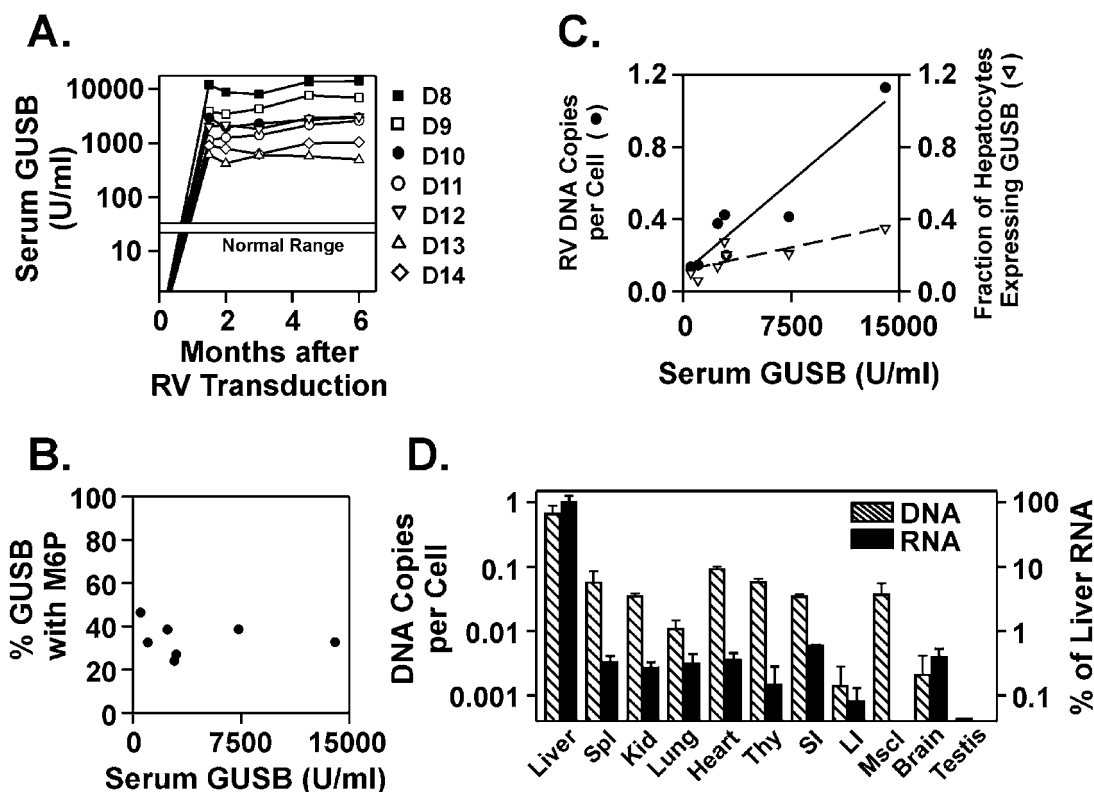


**FIG. 1.** Serum GUSB activity and transduction efficiency in RV-treated mice. (A) Serum GUSB activity. MPS VII mice were injected with  $1 \times 10^{10}$  rfu/kg of HAAT-cGUSB-WPRE at 3 days after birth. Serum was tested for GUSB activity at the indicated times after transduction. The values at 0 months (0.04 U/ml) represent those present in adult untreated MPS VII mice. The average values in homozygous normal mice ( $28 \text{ U/ml} \pm 2 \text{ SD}$ ) are indicated by the boxed region. D8, D9, D11, and D12 were male, and D10, D13, and D14 were female. (B) Percentage serum GUSB with M6P. The percentage of GUSB that contained M6P was determined for serum samples obtained at 6 months after birth and are plotted vs the average serum GUSB activity in the same animal. (C) Transduction efficiency in liver. DNA was isolated from liver at 6 months after transduction and analyzed for RV DNA sequences using real-time PCR. The copies of RV per diploid genome were plotted vs the serum GUSB level for the same animal. The fraction of hepatocytes that expressed GUSB was determined by analysis of liver sections after histochemical staining for GUSB activity. Two nontransduced MPS VII mice had no detectable RV DNA sequences ( $<0.002$  copies per cell) and no transduced hepatocytes. (D) DNA and relative RNA levels in organs. The average RV DNA copy number per diploid genome  $\pm$  SEM in organs was determined using real-time PCR for the three RV-treated mice with the highest serum GUSB activity. Spl, spleen; Kid, kidney; Thy, thymus; SI, small intestines; LI, large intestines; and MscI, muscle. Only two testes were evaluated, as one animal was female. Note that the average copy number in the liver for these mice is higher than the average obtained using all seven RV-treated mice. The average relative amount of RNA  $\pm$  SEM was determined in organs for three animals with relatively low levels of expression using real-time PCR after reverse transcription (RT) of DNase I-treated RNA. The average level in the liver was defined as 100%. Samples from the liver of RV-treated mice had no signal when real-time PCR was performed without preceding RT, and samples from nontransduced mice had no signal after RT and PCR (not shown). Testis was not evaluated for RNA levels as all animals were female.

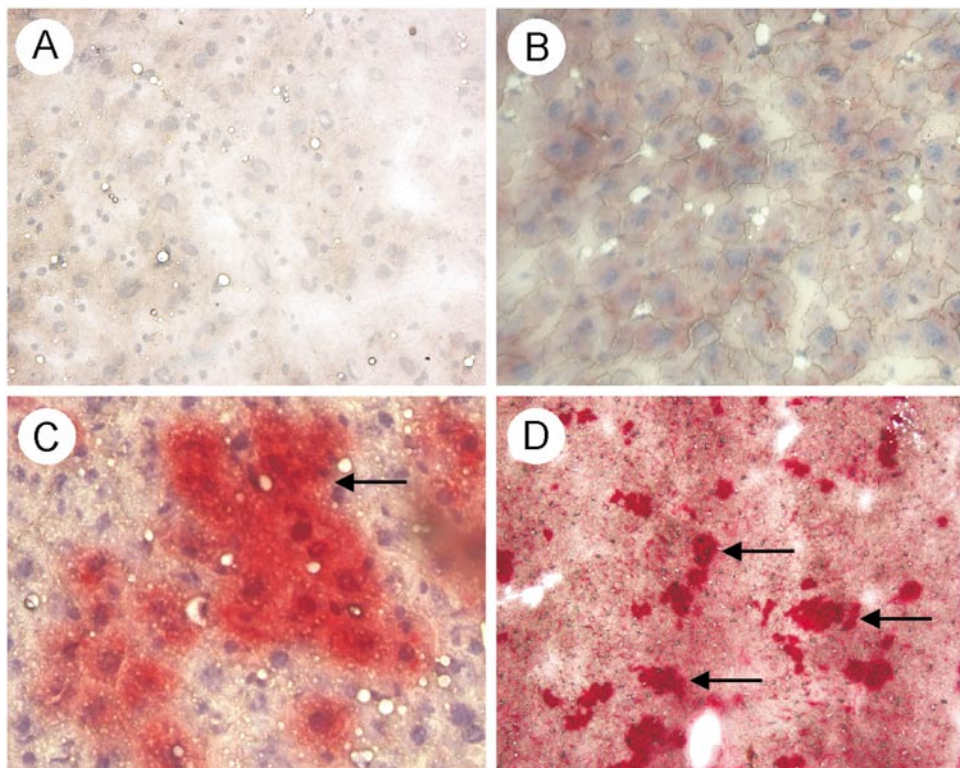
tivity was due to contaminating blood. The average liver GUSB activity was  $1664 \pm 570 \text{ U/mg}$  (8.7-fold normal) (Fig. 3A). In addition, total  $\beta$ -hexosaminidase ( $\beta$ -Hex) activity was determined, as activity for these enzymes is elevated in MPS VII, and normalization indicates effective treatment. For the RV-treated mice, liver  $\beta$ -Hex levels were significantly lower than in untreated MPS VII mice ( $P = 0.0007$ ) and were indistinguishable from those in normal mice ( $P = 0.98$ ). This suggests that the GUSB levels were sufficient to reduce this secondary effect of lysosomal storage in the liver.

GUSB activity in other organs from RV-treated mice is presented in Fig. 3A in order from highest to lowest specific activity. In spleen, lung, thymus, large intestine,

kidney, heart, and muscle, GUSB activity was significantly higher in the RV-treated than in the untreated MPS VII mice ( $P < 0.05$ ) and resulted in a statistically significant reduction in  $\beta$ -Hex activity ( $P < 0.02$  vs values in untreated MPS VII mice). In the small intestines and brain, GUSB activity was not statistically higher in the RV-treated than in the untreated MPS VII mice. Nevertheless,  $\beta$ -Hex activity was normalized for the RV-treated animals in both of these organs ( $P < 0.004$  for RV-treated vs untreated MPS VII mice), suggesting that the GUSB activity that was present was sufficient to reduce lysosomal storage.

The serum GUSB levels were plotted vs the organ activity for individual animals to determine if there was a

**FIG. 2.** Histochemical analysis of liver for GUSB activity. Animals were sacrificed at 6 months of age. Frozen sections were stained for GUSB activity (red in the cytoplasm) and counterstained with hematoxylin (blue for nuclei). (A) MPS VII. After 16 h of GUSB staining, no enzyme activity was present. Original magnification 60 $\times$ . (B) Normal. After 1 h of GUSB staining there was little activity in the hepatocytes. Original magnification 60 $\times$ . (C and D) RV-treated mouse with low serum GUSB activity. For an RV-treated MPS VII mouse with low serum GUSB activity (D14), many hepatocytes had high levels of GUSB activity (arrow) after a 1-h stain (C original magnification 60 $\times$ ). A 16-h stain demonstrated that there were numerous clusters of hepatocytes with high GUSB activity, and the entire liver had some activity (D original magnification 10 $\times$ ).



linear relationship (Fig. 3B). Serum GUSB activity was directly proportional to the liver GUSB ( $R^2 = 0.82$ ), which suggests that secretion of enzyme from the liver does not become saturated even with very high levels of expression. There was also a good linear relationship ( $R^2$  between 0.93 and 0.88) between serum GUSB and organ activity in spleen, kidney, and heart. A moderate linear correlation was seen ( $R^2$  between 0.70 and 0.51) in small and large intestine and in brain. Little or no correlation ( $R^2 < 0.35$ ) was seen in lung, muscle, and thymus.

#### GAG Levels in Liver, Spleen, and Kidney

Cells that are deficient in GUSB activity cannot degrade dermatan, heparan, and chondroitin sulfates, which results in an overall elevation in sulfated GAG levels. Liver, spleen, and kidney sulfated GAG levels in the RV-treated mice were statistically lower than in untreated MPS VII mice ( $P < 0.0004$ ) and were indistinguishable from values in normal mice (Fig. 3C). All RV-treated mice had similar normalization of sulfated GAG levels in these organs (not shown).

#### Histochemical and Pathological Analysis of Enzyme Activity and Lysosomal Storage in Organs

We analyzed organs from seven RV-treated MPS VII mice, three age-matched untreated MPS VII mice, and two age-matched homozygous normal mice by histochemistry for GUSB enzyme activity and by toluidine blue staining of

1- $\mu$ m sections for evidence of lysosomal storage. Representative examples of GUSB staining and histopathological analyses are shown for kidney (Figs. 4A to 4D), small intestines (Figs. 4E and 4F), heart (Figs. 5A and 5B), aorta (Figs. 5C and 5D), lung (Figs. 5E and 5F), thymus (Figs. 6A to 6C), eye (Figs. 6D to 6F), and brain (Fig. 7).

The severity of lysosomal storage was evaluated for each organ in these animals, as summarized in Table 1. All RV-treated mice had a marked reduction in histopathological evidence of lysosomal storage in liver, spleen, small intestine, kidney glomeruli and cortical tubules, cortical and hippocampal neurons, glial cells, meninges, and perivascular cells of the brain. Most or all RV-treated mice had at least a partial reduction in lysosomal storage in the bronchial epithelium, cortex and medulla of the thymus, medullary tubules of the kidney, heart valve, aorta, corneal stroma, and retinal pigmented epithelium. In most cases, RV-treated mice with high serum GUSB activity had more pathological improvement in these organs than did those with low serum GUSB activity, although the small number of animals analyzed and the variation within groups make it difficult to definitely say that higher serum GUSB activity is better. Six of the seven RV-treated mice analyzed had no improvement in storage material in Purkinje cells. However, D8, the RV-treated mouse with the highest serum GUSB activity, had a marked reduction in lysosomal storage in this cell type.

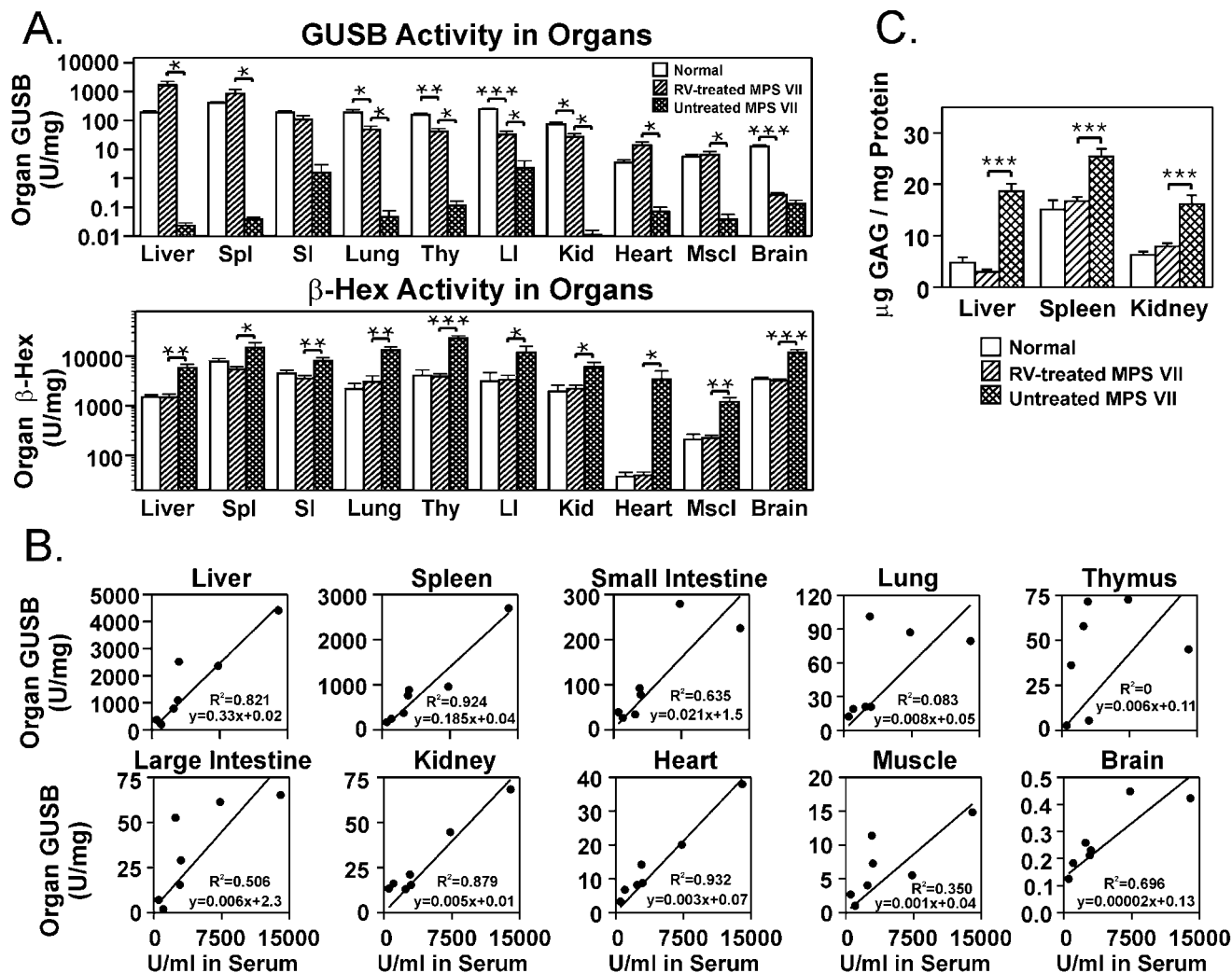


FIG. 3. Lysozymal enzyme activity and GAG levels. (A) GUSB and  $\beta$ -Hex activity in organs. The GUSB and  $\beta$ -Hex activity was determined in homogenates of organs obtained at 6 months after transduction and averages  $\pm$  SEM were determined. Abbreviations are as in Fig. 1. Statistical comparisons between values from normal ( $N = 5$ ) and RV-treated ( $N = 7$ ) mice are shown above the bracket that joins the two bars, where \* represents a  $P$  value of 0.05 and 0.005, \*\* represents a  $P$  value of 0.005 and 0.0005, and \*\*\* represents a  $P$  value  $< 0.0005$ . No value is indicated if the  $P$  value is  $> 0.05$ . Statistical comparisons between values from RV-treated and untreated MPS VII ( $N = 5$ ) mice are shown in the same fashion. (B) Relationship between serum and organ enzyme activity. The organ GUSB activity in individual RV-treated mice was plotted vs the serum GUSB activity for the same animal. For each organ, the linear regression equation and the  $R^2$  values obtained using these data and a  $y$  intercept that represents the GUSB enzyme activity in untreated MPS VII mice are shown. (C) Sulfated GAG levels were plotted as the average  $\pm$  SEM, and statistical comparisons between normal ( $N = 5$ ) and RV-treated ( $N = 7$ ) mice and between RV-treated mice and untreated MPS VII ( $N = 5$ ) mice are as described in A.

## DISCUSSION

### Neonatal iv Injection of RV Results in Stable Transduction of Hepatocytes

In this study, a simple iv injection of RV at 3 days after birth resulted in stable transduction of hepatocytes, as  $19 \pm 3.8\%$  contained high enzyme activity, and there were  $0.40 \pm 0.13$  copies of the RV per diploid genome in the liver at 6 months. A similar ratio of approximately 2 copies of RV per histochemically apparent transduced hepatocyte was observed in neonatal canine hepato-

cytes at 5 days after transduction [28]. The higher number of RV DNA copies per cell in the liver versus the percentage of hepatocytes with high-level expression may be due to multiple transductions per cell, no or low expression in some transduced hepatocytes, or transduction of nonparenchymal cells. We conclude that each transduced hepatocyte has few copies of the RV. Since several mutations are required for the development of cancer, this should reduce the chance of insertional mutagenesis leading to malignant transforma-

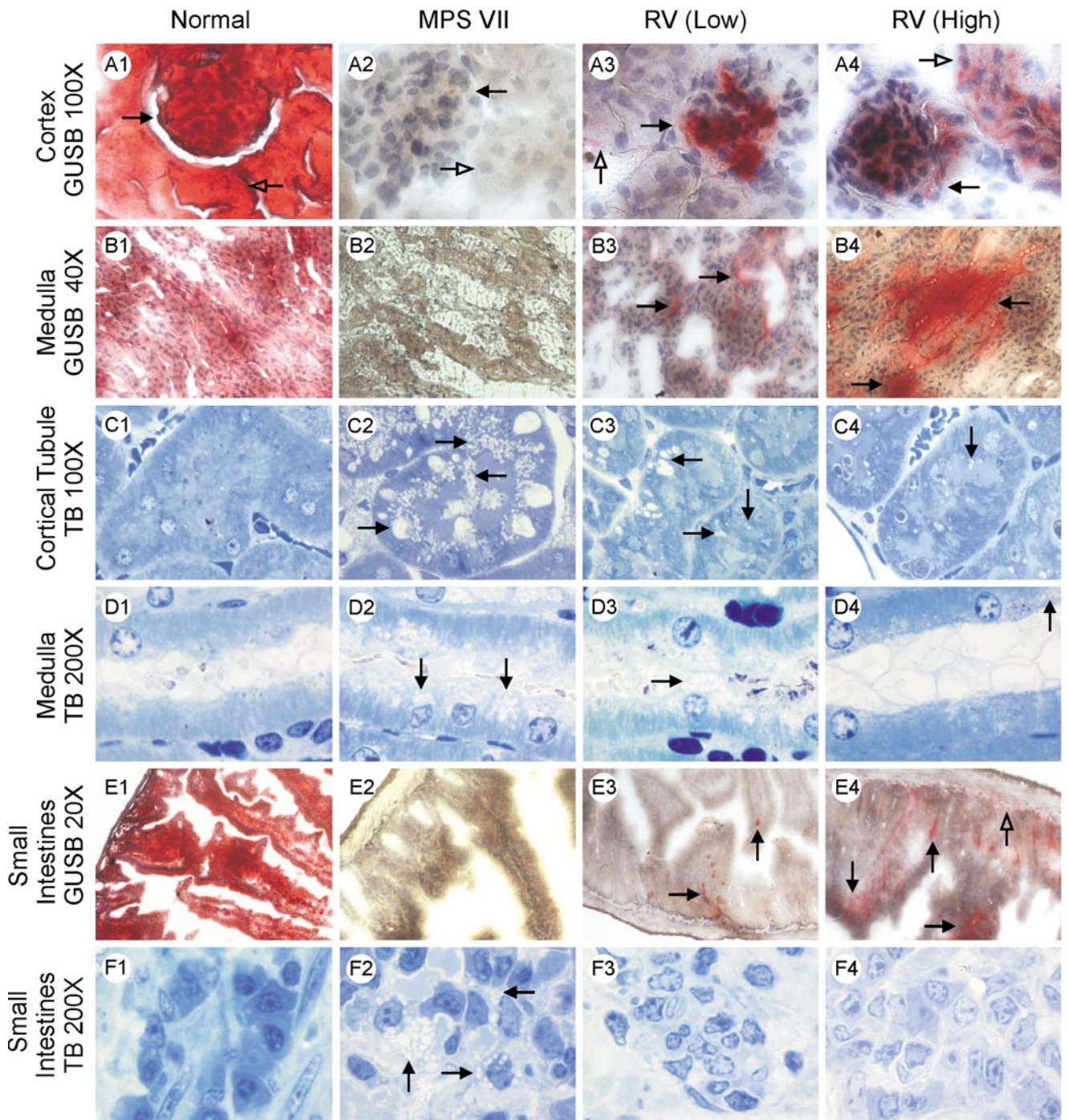


**FIG. 4.** Evaluation of kidney and small intestine. GUSB staining was performed for 16 h followed by counterstain with hematoxylin. Histopathological analysis involved staining of 1- $\mu$ m sections with toluidine blue (TB), and arrows in these images identify lysosomal storage material. Normal mice (images labeled with 1), untreated MPS VII mice (labeled with 2), RV-treated mice with low serum GUSB activity (labeled with 3), and RV-treated mice with high serum GUSB activity (labeled with 4) were sacrificed at 6 months of age. The original magnification is shown at the left of each row. (A) GUSB stain of kidney cortex. Black arrows identify glomeruli, and open arrows identify tubules. (B) GUSB stain of the kidney medulla. Black arrows identify cells with GUSB activity. (C) Histopathology of kidney cortical tubules. The pathological scores for lysosomal storage were 0, +, +, +, and +, for 1, 2, 3, and 4, respectively. (D) Histopathology of kidney medulla. The pathological scores for lysosomal storage were 0, +, +, +, and +, for 1, 2, 3, and 4, respectively. (E) GUSB stain of small intestines. Black arrows identify enzyme activity in the lamina propria of the small intestines of RV-treated MPS VII mice, while the open arrow identifies enzyme activity in the submucosa. (F) Histopathology of the lamina propria of the small intestines. The pathological scores for lysosomal storage were 0, +, +, 0, and 0, for 1, 2, 3, and 4, respectively.

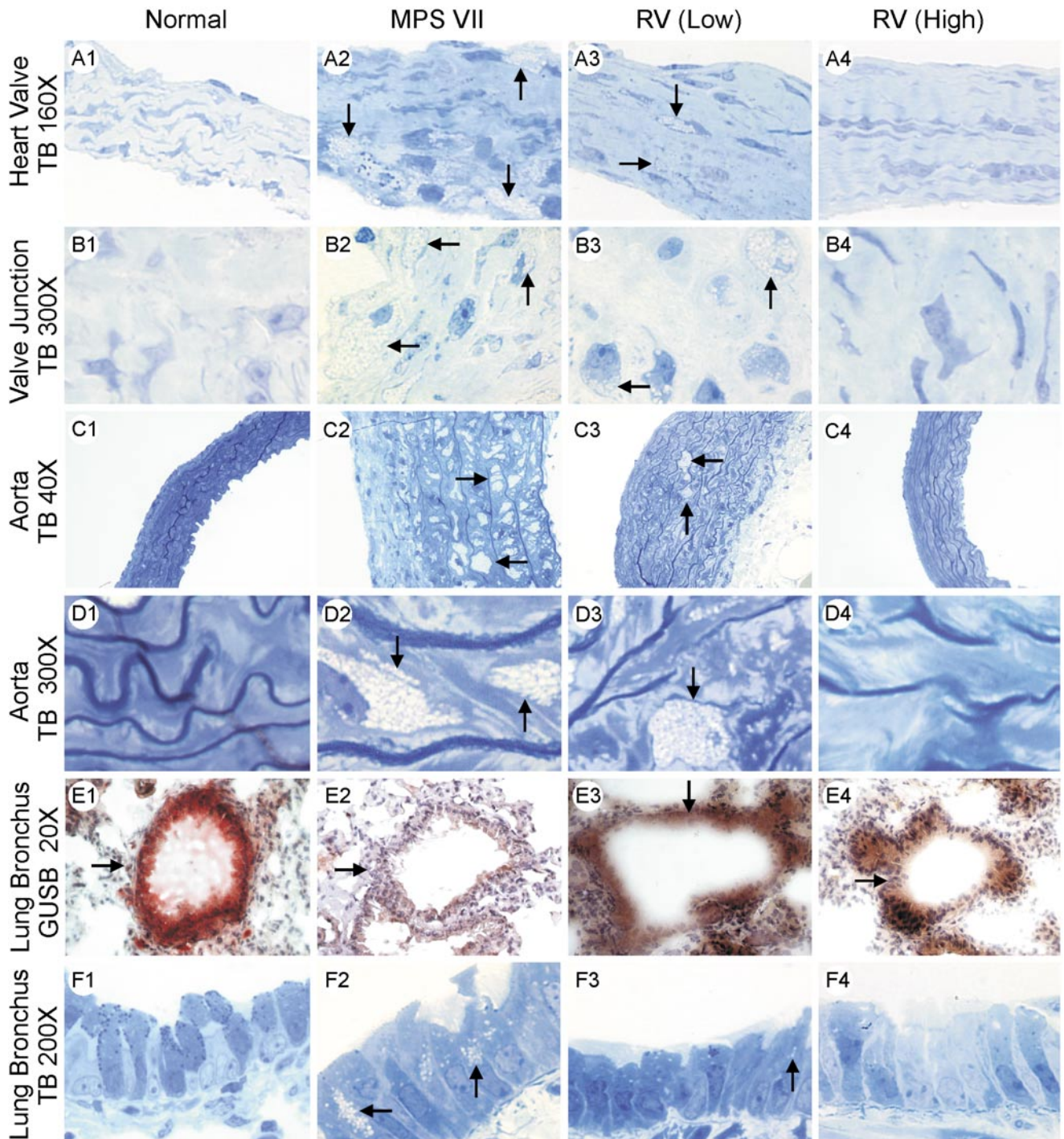
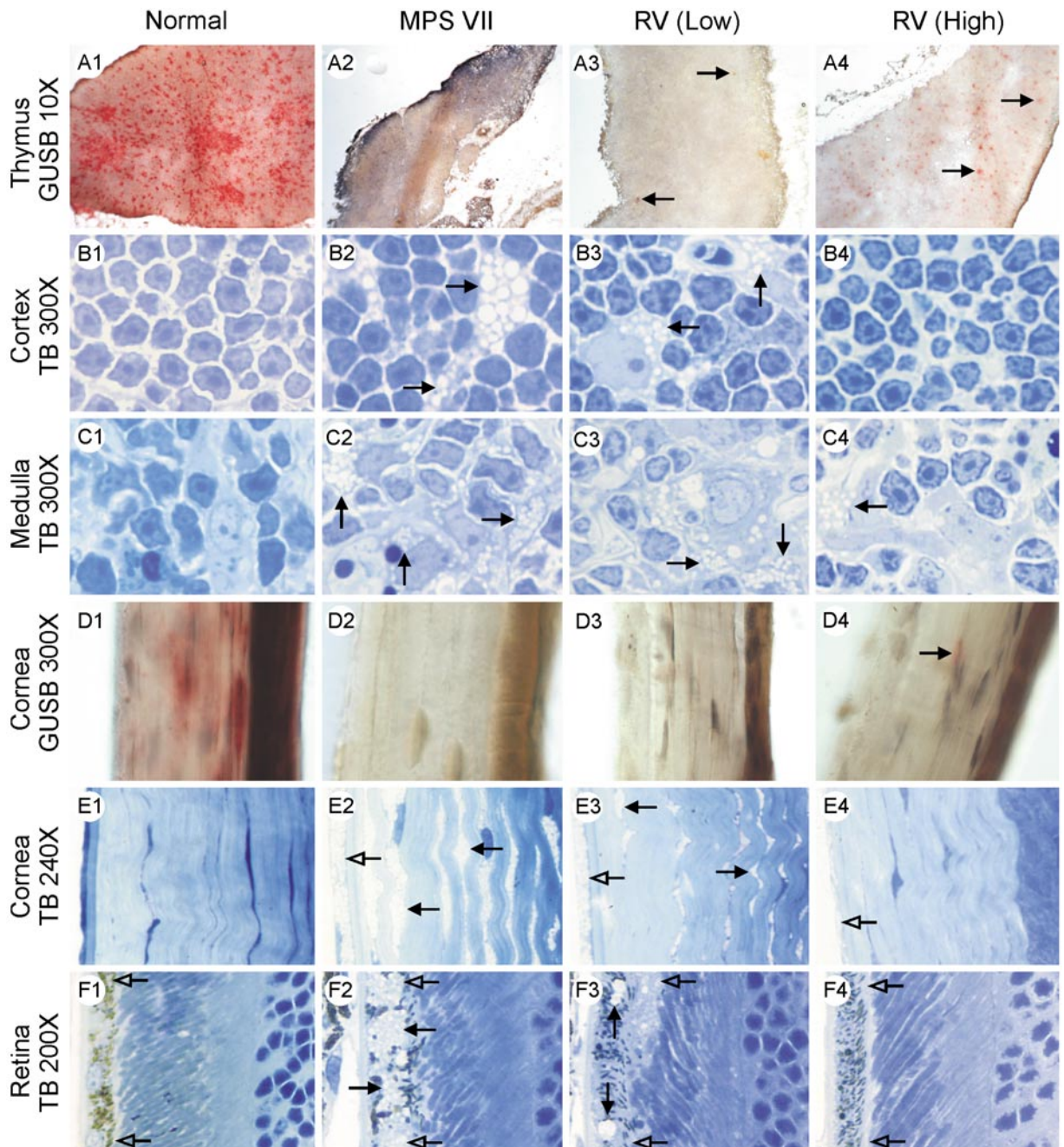


FIG. 5. Evaluation of heart, aorta, and lung. Groups are identified and GUSB and toluidine blue (TB) staining were done as described for Fig. 4. For all images that involve histopathological analysis with TB staining, arrows identify lysosomal storage material. (A) Histopathology of the aortic valve leaflet. The pathological scores for lysosomal storage were 0, +, +, +, +, +, and 0, for 1, 2, 3, and 4, respectively. (B) Histopathology of the aortic valve attachment region. Arrows identify lysosomal storage material in the region where the aortic valve leaflet attaches to the heart. The pathological scores for lysosomal storage were 0, +, +, +, +, +, +, and 0, for 1, 2, 3, and 4, respectively. (C and D) Histopathology of aorta. The pathological scores for lysosomal storage were 0, +, +, +, +, +, +, and 0, for 1, 2, 3, and 4, respectively. (E) GUSB staining of lung bronchi. Arrows identify the bronchi. (F) Histopathology of the bronchial epithelium of the lung. The pathological scores for lysosomal storage were 0, +, +, +, +, +, +, and 0, for 1, 2, 3, and 4, respectively.



**FIG. 6.** Evaluation of thymus and eye. Groups are identified, and GUSB and toluidine blue (TB) staining were done as described for Fig. 4. For all histopathology with toluidine blue staining, arrows identify lysosomal storage material. (A) GUSB stain of thymus. Arrows identify GUSB activity in the cortex of the thymus of RV-treated mice. (B) Histopathology of the thymus cortex. The pathological scores for lysosomal storage were 0, +, ++, +, and 0, for 1, 2, 3, and 4, respectively. (C) Histopathology of the thymus medulla. The pathological scores for lysosomal storage were 0, +, ++, +, and 0, for 1, 2, 3, and 4, respectively. (D) GUSB stain of the cornea. The arrow identifies GUSB activity in the cornea of a RV-treated mouse. (E) Histopathology of the cornea. Black arrows identify lysosomal storage material in the stroma of the cornea, and open arrows identify storage in the corneal endothelium. The pathological scores for lysosomal storage in the stroma were 0, +, ++, +, and 0, for 1, 2, 3, and 4, respectively. (F) Histopathology of retina. For all images, open arrows identify the right edge of the pigmented retinal epithelium, while black arrows identify lysosomal storage. The pathological scores for lysosomal storage were 0, +, ++, +, and 0, for 1, 2, 3, and 4, respectively.

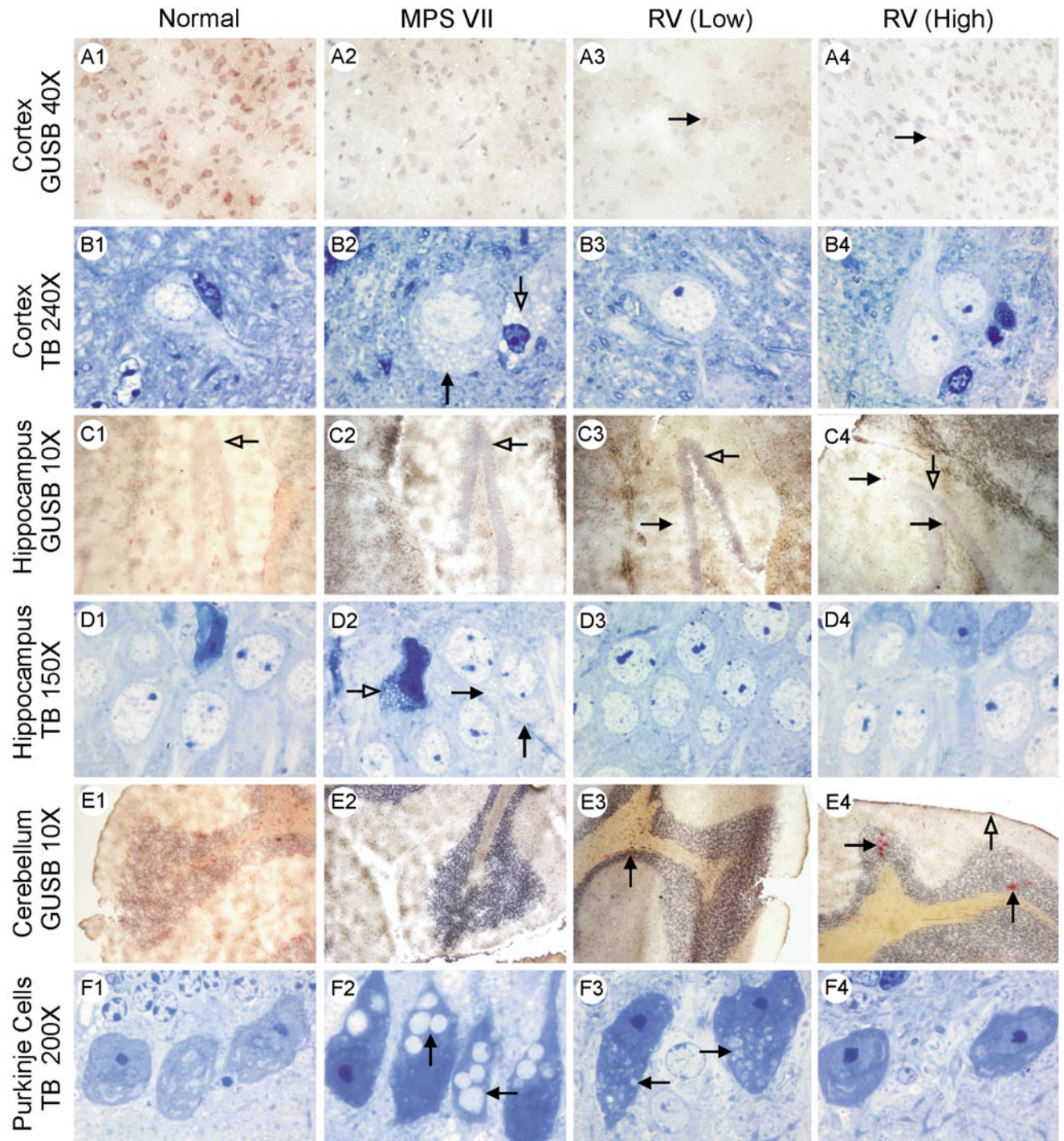


FIG. 7. Evaluation of brain. Groups are identified, and GUSB and toluidine blue (TB) staining were done as described for Fig. 4. (A) GUSB stain of brain cortex. Arrows identify cells in the cortex of RV-treated mice that contain GUSB activity. (B) Histopathology of brain cortex. Black and open arrows identify storage material within a neuron and a glial cell, respectively. The pathological scores for lysosomal storage were 0, +, +, +, +, 0, and 0, for 1, 2, 3, and 4, respectively. (C) GUSB stain of hippocampus. The black arrows identify cells with enzyme activity, while open arrows identify the hippocampus. (D) Histopathology of hippocampus. Black and open arrows identify lysosomal storage in neurons and a glial cell, respectively. The pathological scores for lysosomal storage were 0, +, +, +, +, 0, and 0, for 1, 2, 3, and 4, respectively. (E) GUSB stain of cerebellum. Arrows identify cells in the granular layer with GUSB activity, while the open arrow identifies enzyme activity in the meninges. (F) Histopathology of cerebellum. Arrows identify lysosomal storage in Purkinje cells. The pathological scores for lysosomal storage were 0, +, +, +, +, +, +, +, and 0, for 1, 2, 3, and 4, respectively.

**TABLE 1:** Summary of effect of RV-mediated gene therapy upon pathology in MPS VII mice

Organ	Cell type or region	Normal mice (N = 2)	Untreated MPS VII mice (N = 3)	RV-treated MPS VII mice		
				Low serum GUSB	Medium serum GUSB	High serum GUSB
Liver	Hepatocytes	0	++++	0	0	0
	Sinus lining cells	0	++++	0	0	0
Spleen	Red pulp	0	++++	0 <sup>a</sup>	0	0
Small intestine	Lamina propria	0	++	0	0	0 <sup>a</sup>
	Submucosa	0	+, +, +++++	0	0	0 <sup>a</sup>
Lung	Bronchial cells	0	++++	+	+, 0	0 <sup>a</sup>
Thymus	Cortex	0	+++ <sup>a</sup>	++, +	+ <sup>a</sup>	0 <sup>a</sup>
	Medulla	0	+++ <sup>a</sup>	+++ , ++	++ , +	+ <sup>a</sup>
Kidney	Glomeruli	0	++++	0	0	0
	Cortical tubules	0	++++	+	+	+
	Medullary tubules	0	++++ , ++	++ , +	+, + , 0	+ <sup>a</sup>
Heart	Valve	0	++++	+	+, + , 0	0 <sup>a</sup>
	Valve attachment area	0	++++ <sup>a</sup>	+++ , ++	++++ , ++ , ++	0 <sup>a</sup>
Aorta	Media	0	++++	+++	+, +++	+, 0
Eye	Corneal stroma	0	++++ <sup>a</sup>	++	++ , + , 0	0
	Retinal pigmented epithelium	0	++++ <sup>a</sup>	++	++ , + , 0	+, 0
Brain	Cortical neurons	0	++++	0	0	0
	Hippocampal neurons	0	++++	0	0	0
	Purkinje cells	0	++++	++++	++++	++++ , 0
	Glial cells	0	++++	0	0	0
	Meninges	0	++++	0	0	0
	Perivascular cells	0	++++	0	0	0

The severity of pathologic changes consistent with lysosomal storage disease was determined for organs or cell types from normal, untreated MPS VII, or RV-treated MPS VII mice with low (581 or 947 U/ml), medium (1844, 2733, or 2890 U/ml), or high (5649 or 10070 U/ml) serum GUSB activity. 0 represents histology that is indistinguishable from normal; + represents animals in which storage was absent in some fields and present in others; ++ represents animals in which storage was present in all fields, but at low levels; +++ represents animals in which storage was present in all fields at moderate levels; ++++ represents animals with large amounts of storage material in all fields. In some organs, the untreated MPS VII mice had only low amounts of storage material. Unless otherwise indicated, results from all of the samples of a particular organ and group were concordant.

<sup>a</sup>Only one of two animals, or only two of three animals, of the group were evaluated, and values were concordant if more than one animal was evaluated. For results that were discordant within the group, the results for each animal that was evaluated are shown.

tion over that observed if each transduced cell had many integrations.

The percentage of hepatocytes that expressed the cGUSB cDNA at high levels in the RV-treated MPS VII mice (19%) was ninefold higher than after iv injection of the same vector into neonatal MPS VII dogs (2.1%) [28]. This may be due to the threefold higher dose of RV per kilogram used in mice compared with the canine study. Alternatively, there may be a higher percentage of replicating hepatocytes in neonatal mice than in dogs, although this has not yet been tested experimentally. There was an eightfold variation in the copies of RV per cell in the liver among individual animals. This may reflect variation in the number of replicating hepatocytes in individual animals, since cell division is necessary for transduction with an MLV-based RV.

The liver was the major target organ for long-term transduction, as the DNA copy number was greater than sevenfold higher than in any other organ at 6 months. The maintenance of a high copy number despite a substantial increase in size is likely the result of clonal expansion of hepatocytes during normal postnatal growth [31]. Since the cluster size observed at 6 months after transduction was similar to what was observed in transgenic mice that expressed  $\beta$ -galactosidase in a subset of hepatocytes beginning shortly after birth [32], we do not believe that transduction conferred abnormal growth properties upon the hepatocytes. However, further studies will be performed to determine if some transduced cells proliferate abnormally. Although splenocytes were transduced as efficiently as liver cells when DNA analysis was performed 5 days after injection of an RV into neonatal dogs [28], the

copy number was only 8% of that in liver at 6 months after transduction in mice. This decline in spleen may be due to the limited life span of splenocytes. Since other organs had low RV DNA and RNA levels relative to those in liver, most of the enzyme activity in other organs was probably taken up from blood, although it remains possible that some enzyme was derived from expressing cells.

### The Liver Secretes GUSB with M6P

Serum GUSB activity for RV-treated mice was stable for 6 months at 3531 U/ml (127-fold normal), which exceeds the highest long-term expression of GUSB from an AAV vector (~300 U/ml) [21]. Although the peak serum GUSB activity was higher (~9000 U/ml) after administration of an adenoviral vector, levels fell over time [24]. The serum GUSB contained normal amounts of M6P, demonstrating that the addition of M6P was not saturated by the over-expression of GUSB in hepatocytes. The level of mannose-6-phosphorylated GUSB in serum varied from 269 U/ml for D13 to 3291 U/ml for D8. If one assumes that the half-life of mannose-6-phosphorylated canine GUSB is 10 min based upon data with murine GUSB in mice [22], and that the serum volume of mice in liters is 4% of the body weight in kilograms, it can be calculated that D13 and D8 would secrete at least 1.8 million and 22 million units of phosphorylated enzyme per kilogram per week, respectively. For comparison, mice that started ERT shortly after birth received 28 million units/kg for their first dose, followed by lower doses on a per kilogram basis (~1.4 million units/kg at 6 weeks) as they grew in size, but still received a constant amount of enzyme [10–14].

Serum levels of 269 and 3291 U/ml phosphorylated GUSB would correspond to 0.22 and 2.8 nM, respectively, if one assumes a specific activity for phosphorylated enzyme of  $4 \times 10^6$  U/mg [12] and a molecular weight of the tetramer of 300 kDa. Since the affinity of the cationic-independent M6PR for uptake of diphosphorylated oligosaccharides is 2 nM [9] and the enzyme concentration is likely lower in tissues than in blood, uptake should not be saturated at these levels. Indeed, organ activity correlated reasonably well with serum GUSB activity in spleen, small intestine, large intestine, kidney, heart, and brain. It is unclear why there was a poor correlation ( $R^2$  less than 0.5) between serum and organ GUSB activity in lung, thymus, and muscle.

### No Immunological Response to cGUSB Was Detected

Gene therapy might induce antibody or cytotoxic T lymphocyte (CTL) responses that would prevent secreted protein from reaching other organs or destroy transduced cells, respectively. In this study, none of the sera from RV-treated mice contained anti-cGUSB IgG antibodies that could be captured by an ELISA plate that was coated with 5 µg/ml purified cGUSB (data not shown). Similarly, no anti-human GUSB (hGUSB) antibodies were detected after neonatal injection of an AAV vector into muscle

[33]. In contrast, anti-hGUSB antibodies developed after injection of hGUSB protein [34] or gene therapy to adult mice with hGUSB-expressing retroviral [17] or adenoviral [24] vectors. In addition, anti-murine GUSB (mGUSB) antibodies developed in MPS VII mice that received transduced fibroblasts [35], although they did not develop in mice that received injections of mGUSB protein beginning shortly after birth or as young adults [13]. A significant CTL response did not occur here since transduced cells clearly survived and maintained high expression levels for 6 months. Thus, neonatal gene therapy approaches may induce tolerance to GUSB.

### Effect of Gene Therapy upon Organ Pathology

This gene therapy approach resulted in a marked reduction in lysosomal storage in liver, spleen, and kidney glomeruli of RV-treated MPS VII compared with untreated MPS mice, which is consistent with the results of others demonstrating that it is relatively easy to correct pathological storage in these sites even with low levels of enzyme activity [16]. In contrast, histopathological correction of tubular storage material in the kidney has been variable and has required either high serum levels of GUSB or bone marrow transplant (BMT) [17,24,36,37]. The fact that animals with higher serum activity had more histochemical staining for GUSB activity in the tubules than did animals with lower expression in this study is consistent with the hypothesis that high serum levels are required for delivery of a lysosomal enzyme to the tubules, which may have implications for Fabry disease. The presence of GUSB and reduction in lysosomal storage material in the small intestines may have implications for Wolman disease, which is a lysosomal storage disease that is associated with gastrointestinal symptoms. The presence of GUSB and reduction in lysosomal storage in the bronchi may have implications for lung disease in MPS syndromes, although lung disease has generally been attributed to upper airway disease [2,3]. The presence of GUSB and reduction in lysosomal storage in the thymus may have implications for the immune defect that occurs in MPS VII [38]. The reduction in storage material in the heart valves in this study is important, as heart disease is a major cause of death in MPS syndromes. Our results are consistent with the effect of AAV-mediated gene therapy in mice [20] and with echocardiographic improvements in RV-treated MPS VII dogs [29]. In addition, BMT to adult MPS VII mice improved pathology in the heart valves [37]. However, this approach may have advantages over other treatments for arterial disease, as substantial correction of pathological abnormalities was achieved in the aortic media here, but did not occur with ERT beginning shortly after birth or BMT to adult mice [11,37].

Eye and neurological symptoms are important manifestations of MPS VII. The reduction in the amount of storage material in the cornea here is consistent with the reduction in cornea clouding observed on clinical exam-

ination in MPS VII dogs that received RV-mediated neonatal gene therapy [29]. This result is similar to what was observed after BMT [37], although surprisingly ERT was ineffective in the cornea [11–13]. The pathological improvements in the pigmented retinal epithelium are similar to what occurred after ERT [13], BMT [39], and systemic AAV vector-mediated gene therapy [20] and will likely correlate with improvements in retinal function [21,40]. The relatively small amounts of GUSB activity in the brain of RV-treated mice was sufficient to normalize  $\beta$ -Hex activity and prevent accumulation of lysosomal storage material in cortical and hippocampal neurons, glial cells, perivascular cells, and the meninges for all RV-treated mice. Similar improvements were observed in MPS VII mice after systemic neonatal AAV-mediated gene therapy [20]. ERT alone or in combination with BMT resulted in improvements in all of these regions except for glial cells [11–13], while BMT alone to adults failed to improve pathology in neurons or glial cells [37] in MPS VII mice. For the RV-treated mouse with the highest serum GUSB activity, storage was also reduced in Purkinje cells of the cerebellum, a cell type that has been resistant to correction with other treatments, although none of the other mice had reduced storage in Purkinje cells. The pathological improvements observed here will likely result in neurological improvements based upon results with other treatments [16,41–43]. However, since the GUSB activity present in brain likely derived from enzyme that entered from blood prior to the development of the blood–brain barrier, systemic gene therapy might need to be combined with a brain-directed approach for long-term benefit.

### Implications for Gene Therapy

The goal of this study was to identify a target level of serum GUSB for preventing the development of clinical symptoms in MPS VII without adverse effects. Since animals with low serum GUSB activity had at least partial improvements in most pathological abnormalities, achieving long-term expression of  $\sim 500$  U/ml GUSB in serum is a reasonable target. This is consistent with results obtained after AAV-mediated gene therapy in mice, in which serum activity that was  $\sim 300$  U/ml had a marked effect upon many pathological and clinical parameters of disease [21]. Our results are also consistent with gene therapy experiments in MPS VII dogs, in which achieving 195 U/ml resulted in marked improvements in mobility, cardiac disease, and eye disease for up to 14 months [29]. In this study, higher GUSB expression (5000 to 10,000 U/ml in serum) appeared to result in less lysosomal storage in heart valves, aorta, thymus, bronchial epithelium, and eye compared with RV-treated animals with low serum GUSB activity. In addition, the animal with the highest level of serum GUSB activity had reduced storage in Purkinje cells, which has not been improved in previous experiments. However, animals with higher serum GUSB

activity have a greater percentage of transduced hepatocytes and may be at increased risk for the development of cancer over those with lower expression. Future experiments will determine if these additional pathological improvements in animals with higher serum GUSB activity will be consistently observed when more animals are analyzed and if they will result in a more profound clinical effect compared with that which occurs in RV-treated mice with low serum GUSB activity. In addition, studies are in progress to determine if RV-treated MPS VII mice develop tumors. These studies should help to define the target serum GUSB activity for treating patients with systemic gene therapy.

## MATERIALS AND METHODS

**Animal procedures.** MPS VII mice and homozygous normal controls in a B6.C-H-2<sup>bm1</sup> background were maintained in a pathogen-free environment on a diet with 11% fat (PicoLab Mouse Chow 20 5058). Three-day-old MPS VII mice were injected via the temporal vein with 100  $\mu$ l of hAAT-cGUSB-WPRE containing  $1 \times 10^7$  rfu, for a dose of  $1 \times 10^{10}$  rfu/kg. hAAT-cGUSB-WPRE has been described previously [28] and 8  $\mu$ g/ml Polybrene (final concentration) was added just prior to injection. Serum was obtained by retro-orbital bleeding.

**Analysis of GUSB activity and GAG levels.** Eight-micrometer frozen sections were fixed and stained for GUSB activity with 0.25 mM naphthol AS-BI- $\beta$ -D-glucuronide as described [44] except for the following modification. Liver sections were fixed at 25°C for 20 min to reduce the enzyme activity and stained for 1 to 16 h. Sections from other organs were fixed at 4°C for 20 min and stained for 16 h. To obtain the percentage of transduced hepatocytes, the number of large intensely red cells per high-power field after a short GUSB stain was divided by the total number of hepatocytes, as detailed previously [28]. For quantification of GUSB activity, 5  $\mu$ l of serum or  $\sim 25$   $\mu$ g of organ homogenate was incubated with 5 mM 4-methylumbelliferyl  $\beta$ -D-glucuronide (Sigma Chemical, St. Louis, MO) for 1 to 16 h, and the fluorescence was measured [44]. One unit of enzyme activity releases 1 nmol of 4-methylumbelliferone per hour. Samples with high activity were diluted. GUSB activity was normalized to total protein as determined with the Bradford assay (Bio-Rad Laboratories, Hercules, CA). The percentage of enzyme that contained M6P was determined using a M6PR column as described previously [29]. Total  $\beta$ -Hex activity was determined using 4 mM 4-methylumbelliferyl-2-acetamido-2-deoxy- $\beta$ -glucopyranoside as the substrate. GAGs were measured by the alcian blue method [45] and normalized to milligrams of protein present in the sample. Statistical comparisons between two groups used the Student *t* test within the program Quattro Pro (Corel Corp., San Diego, CA).

**Pathological analysis of organs.** Samples were fixed as detailed previously and 1- $\mu$ m sections were stained with toluidine blue [5]. Organs were evaluated for lysosomal storage by M.S.S., who was blinded as to the genotype and treatment status of animals. Uncertainties were referred to a pathologist. For most organs, all regions of 10 sections were examined at 40 $\times$  magnification and at higher power if necessary. For the heart valve and bronchial epithelium, fewer fields were evaluated in some animals due to insufficient amounts of tissue with the cells of interest. A failure to analyze an organ from an animal was due to the absence of the region of interest on the slide or to loss of the organ by the pathology department.

**PCR for detection of RV DNA and RNA sequences.** DNA was isolated from organs in a room distant from the main laboratory and real-time PCR was performed on 100 ng of DNA using Taqman technology (Applied Biosystems, Rockville, MD) [28]. DNA from nontransduced MPS VII mice was isolated and amplified at the same time to demonstrate a lack of contamination. Samples were heated to 95°C for 10 min, and then 40 cycles of PCR were performed with 15 s at 95°C and 1 min at 60°C. The WPRE

reaction used primers from nt 1448 to 1467 of the top (5'-GGCTGTT-GGGCACTGACAAT-3') and nt 1546 to 1530 of the bottom (5'-ACGTC-CCGCGCAGAATC-3') strand, and the Taqman probe was from nt 1498 to 1520 (5'-TTTCCATGGCTGCTCGCCTGTGT-3') [46]. Real-time PCR was performed for the mouse  $\beta$ -actin gene for normalization purposes with primers from nt 195 to 217 of the top (5'-GACCCTGAAGTACCCATT-GAAC-3') and nt 286 to 265 of the bottom (5'-CACGCACTCATTGTA-GAAGGT-3') strand and a Taqman probe from nt 224 to 252 (5'-TTGT-TACCAACTGGGACGACATGGAGAAG-3') [47]. Standards were created by infecting the murine GUSB-deficient fibroblasts (3521 cells [44]) with hAAT-cGUSB-WPRE at a multiplicity of infection of 0.05 and isolating a single colony with enzyme activity. DNA from these cells was mixed with DNA from normal mice to create standards with 0.5 copy or fewer of the RV DNA per diploid genome. For analysis of other organs, DNA was isolated from three mice with relatively high levels of expression (D8, D9, and D10). To determine the relative amount of RV RNA, real-time RT-PCR was used. RNA was isolated from organs of animals with relatively low levels of expression (D11, D12, and D14) as described [17], and 5 to 20  $\mu$ g was treated with 10 units of RQ1 RNase-free DNase (Fisher Scientific) followed by phenol:chloroform extraction and ethanol precipitation. For each sample, 1.5  $\mu$ g of RNA was used for reverse transcription with the SuperScript First-Strand Synthesis System (Invitrogen, Carlsbad, CA) and the bottom-strand primers of the WPRE and mouse  $\beta$ -actin sequences noted above. Real-time PCR was performed with 1  $\mu$ l of the 20- $\mu$ l RTase reaction using the SYBR green dye kit (Applied Biosystems) and the primers noted above, and the difference in the cycle at which the threshold was reached ( $C_T$ ) was used to determine the relative amounts of RNA. The limit of detection was a level of RNA that was  $>0.04\%$  of that in liver from RV-treated mice.

#### ACKNOWLEDGMENTS

We thank Marie Roberts for breeding of MPS VII mice and Carole Vogler (St. Louis University School of Medicine) for assistance with pathological analyses. This work was supported by the National Institutes of Health (R01 DK54061 and K02 DK02575 awarded to K.P.P., DK57586 and HD35671 awarded to M.S.S., DK54481 awarded to M.E.H.) and a Washington University Digestive Diseases Research Core Center grant (P30 DK 52574). Robert Mango was supported by an HHMI fellowship and N. Matthew Ellinwood by training grant RR T32-07063.

RECEIVED FOR PUBLICATION AUGUST 12, 2002; ACCEPTED OCTOBER 16, 2002.

#### REFERENCES

- Meikle, P. J., Hopwood, J. J., Clague, A. E., and Carey, W. F. (1999). Prevalence of lysosomal storage disorders. *JAMA* 281: 249–254.
- Neufeld, E. F., and Meunzer, J. (2001). The mucopolysaccharidoses. In *Metabolic and Molecular Basis of Inherited Disease* (C. R. Scriver, A. L. Beaudet, W. S. Sly, and D. Valle, Eds.), pp. 3421–3452. McGraw-Hill, New York.
- Sly, W. S., Quinton, B. A., McAllister, W. H., and Rimoin, D. L. (1973). Beta glucuronidase deficiency: Report of clinical, radiologic, and biochemical features of a new mucopolysaccharidosis. *J. Pediatr.* 82: 249–257.
- Yamada, Y., et al. (1998). Treatment of MPS VII (Sly disease) by allogeneic BMT in a female with homozygous A619V mutation. *Bone Marrow Transplant.* 21: 629–634.
- Birkenmeier, E. H., et al. (1989). Murine mucopolysaccharidosis type VII: Characterization of a mouse with  $\beta$ -glucuronidase deficiency. *J. Clin. Invest.* 83: 1258–1266.
- Ray, J., Scarpinon, V., Laing, C., and Haskins, M. E. (1999). Biochemical basis of the beta-glucuronidase gene defect causing canine mucopolysaccharidosis VII. *J. Hered.* 90: 119–123.
- Fyfe, J. C., et al. (1999). Molecular basis of feline beta-glucuronidase deficiency: An animal model of mucopolysaccharidosis VII. *Genomics* 58: 121–128.
- Sands, M. S., and Birkenmeier, E. H. (1993). A single-base-pair deletion in the beta-glucuronidase gene accounts for the phenotype of murine mucopolysaccharidosis type VII. *Proc. Natl. Acad. Sci. USA.* 90: 6567–6571.
- Kornfeld, S. (1992). Structure and function of the mannose 6-phosphate/insulinlike growth factor II receptors. *Annu. Rev. Biochem.* 61: 307–330.
- Vogler, C., et al. (1993). Enzyme replacement with recombinant beta-glucuronidase in the newborn mucopolysaccharidosis type VII mouse. *Pediatr. Res.* 34: 837–840.
- Sands, M. S., et al. (1994). Enzyme replacement therapy for murine mucopolysaccharidosis type VII. *J. Clin. Invest.* 93: 2324–2331.
- Vogler, C., et al. (1996). Enzyme replacement with recombinant beta-glucuronidase in murine mucopolysaccharidosis type VII: Impact of therapy during the first six weeks of life on subsequent lysosomal storage, growth, and survival. *Pediatr. Res.* 39: 1050–1054.
- Sands, M. S., et al. (1997). Murine mucopolysaccharidosis type VII: Long term therapeutic effects of enzyme replacement and enzyme replacement followed by bone marrow transplantation. *J. Clin. Invest.* 99: 1596–1605.
- Soper, B. W., et al. (1999). Enzyme replacement therapy improves reproductive performance in mucopolysaccharidosis type VII mice but does not prevent postnatal losses. *Pediatr. Res.* 45: 180–186.
- Sands, M. S., et al. (2001). Biodistribution, kinetics, and efficacy of highly phosphorylated and non-phosphorylated beta-glucuronidase in the murine model of mucopolysaccharidosis VII. *J. Biol. Chem.* 276: 43160–43165.
- Vogler, C., et al. (2001). Murine mucopolysaccharidosis VII: Impact of therapies on the phenotype, clinical course, and pathology in a model of a lysosomal storage disease. *Pediatr. Dev. Pathol.* 4: 421–433.
- Gao, C., Sands, M. S., Haskins, M. E., and Ponder, K. P. (2000). Delivery of a retroviral vector expressing human beta-glucuronidase to the liver and spleen decreases lysosomal storage in mucopolysaccharidosis VII mice. *Mol. Ther.* 2: 233–244.
- Stein, C. S., et al. (2001). In vivo treatment of hemophilia A and mucopolysaccharidosis type VII using nonprimate lentiviral vectors. *Mol. Ther.* 3: 850–856.
- Watson, G. L., et al. (1998). Treatment of lysosomal storage disease in MPS VII mice using a recombinant adeno-associated virus. *Gene Ther.* 5: 1642–1649.
- Daly, T. M., Vogler, C., Levy, B., Haskins, M. E., and Sands, M. S. (1999). Neonatal gene transfer leads to widespread correction of pathology in a murine model of lysosomal storage disease. *Proc. Natl. Acad. Sci. USA* 96: 2296–2300.
- Daly, T. M., Ohlemiller, K. K., Roberts, M. S., Vogler, C. A., and Sands, M. S. (2001). Prevention of systemic clinical disease in MPS VII mice following AAV-mediated neonatal gene transfer. *Gene Ther.* 8, 1291–1298.
- Elliger, S. S., Elliger, C. A., Lang, C., and Watson, G. L. (2002). Enhanced secretion and uptake of beta-glucuronidase improves adeno-associated viral-mediated gene therapy of mucopolysaccharidosis type VII mice. *Mol. Ther.* 5: 617–626.
- Ohashi, T., et al. (1997). Adenovirus-mediated gene transfer and expression of human beta-glucuronidase gene in the liver, spleen, and central nervous system in mucopolysaccharidosis type VII mice. *Proc. Natl. Acad. Sci. USA.* 94: 1287–1292.
- Stein, C. S., Ghodsi, A., Derksen, T., and Davidson, B. L. (1999). Systemic and central nervous system correction of lysosomal storage in mucopolysaccharidosis type VII mice. *J. Virol.* 73: 3424–3429.
- Kosuga, M., et al. (2000). Adenovirus-mediated gene therapy for mucopolysaccharidosis VII: Involvement of cross-correction in wide-spread distribution of the gene products and long-term effects of CTLA-4lg coexpression. *Mol. Ther.* 1: 406–413.
- Xia, H., Mao, Q., and Davidson, B. L. (2001). The HIV Tat protein transduction domain improves the biodistribution of beta-glucuronidase expressed from recombinant viral vectors. *Nat. Biotechnol.* 19: 640–644.
- Li, X. K., et al. (2002). Prolongation of transgene expression by coexpression of cytokine response modifier a in rodent liver after adenoviral gene transfer. *Mol. Ther.* 5: 262–268.
- Xu, L., et al. (2002). Transduction of hepatocytes after neonatal delivery of a Moloney murine leukemia virus-based retroviral vector results in long-term expression of  $\beta$ -glucuronidase in mucopolysaccharidosis VII dogs. *Mol. Ther.* 5: 141–153.
- Ponder, K. P., et al. (2002). Therapeutic neonatal hepatic gene therapy in mucopolysaccharidosis VII dogs. *Proc. Natl. Acad. Sci. USA* 99: 13102–13107.
- Gates, G. A., Henley, K. S., Pollard, H. M., Schmidt, E., and Schmidt, F. W. (1961). The cell populations of human liver. *J. Lab. Clin. Med.* 57: 182–184.
- Ponder, K. P. (1996). Analysis of liver development, regeneration and carcinogenesis by genetic marking studies. *FASEB J.* 10: 673–682.
- Kennedy, S. C., Rettlinger, S. D., Flye, M. W., and Ponder, K. P. (1995). Experiments in transgenic mice demonstrate that hepatocytes are the source for postnatal liver growth and do not stream. *Hepatology* 22: 160–168.
- Daly, T. M., et al. (1999). Neonatal intramuscular injection with recombinant adeno-associated virus results in prolonged beta-glucuronidase expression in situ and correction of liver pathology in mucopolysaccharidosis type VII mice. *Hum. Gene Ther.* 10: 85–94.
- Sly, W. S., et al. (2001). Active site mutant transgene confers tolerance to human beta-glucuronidase without affecting the phenotype of MPS VII mice. *Proc. Natl. Acad. Sci. USA* 98: 2205–2210.
- Ross, C. J., Bastedo, L., Maier, S. A., Sands, M. S., and Chang, P. L. (2000). Treatment of a lysosomal storage disease, mucopolysaccharidosis VII, with microencapsulated recombinant cells. *Hum. Gene Ther.* 11: 2117–2127.
- Barker, J. E., et al. (2001). In utero fetal liver cell transplantation without toxic irradiation alleviates lysosomal storage in mice with mucopolysaccharidosis type VII. *Blood Cells Mol. Dis.* 27: 861–873.
- Birkenmeier, E. H., et al. (1991). Increased life span and correction of metabolic defects in murine mucopolysaccharidosis type VII after syngeneic bone marrow transplantation. *Blood* 78: 3081–3092.

38. Daly, T. M., Lorenz, R. G., and Sands, M. S. (2000). Abnormal immune function in vivo in a murine model of lysosomal storage disease. *Pediatr. Res.* **47**: 757–762.
39. Sands, M. S., *et al.* (1993). Treatment of murine mucopolysaccharidosis type VII by syngeneic bone marrow transplantation in neonates. *Lab. Invest.* **68**: 676–686.
40. Ohlemiller, K. K., Vogler, C. A., Roberts, M., Galvin, N., and Sands, M. S. (2000). Retinal function is improved in a murine model of a lysosomal storage disease following bone marrow transplantation. *Exp. Eye Res.* **71**: 469–481.
41. O'Connor, L. H., *et al.* (1998). Enzyme replacement therapy for murine mucopolysaccharidosis type VII leads to improvements in behavior and auditory function. *J. Clin. Invest.* **101**: 1394–1400.
42. Brooks, A. I., *et al.* (2002). Functional correction of established central nervous system deficits in an animal model of lysosomal storage disease with feline immunodeficiency virus-based vectors. *Proc. Natl. Acad. Sci. USA* **99**: 6216–6221.
43. Frisella, W. A., *et al.* (2001). Intracranial injection of recombinant adeno-associated virus improves cognitive function in a murine model of mucopolysaccharidosis type VII. *Mol. Ther.* **3**: 351–358.
44. Wolfe, J. H., and Sands, M. S. (1996). Murine mucopolysaccharidosis type VII: A model system for somatic gene therapy of the central nervous system. In *Protocols for Gene Transfer in Neuroscience: Towards Gene Therapy of Neurological Disorders* (P. R. Lowenstein and L. W. Enquist, Eds.), pp. 264–274. Wiley, New York.
45. Björnsson, S. (1993). Simultaneous preparation and quantitation of proteoglycans by precipitation with alcian blue. *Anal. Biochem.* **210**: 282–291.
46. Zufferey, R., Donello, J. E., Trono, D., and Hope, T. J. (1999). Woodchuck hepatitis virus posttranscriptional regulatory element enhances expression of transgenes delivered by retroviral vectors. *J. Virol.* **73**: 2886–2892.
47. Tokunaga, K., Taniguchi, H., Yoda, K., Shimizu, M., and Sakiyama, S. (1986). Nucleotide sequence of a full-length cDNA for mouse cytoskeletal  $\beta$ -actin mRNA. *Nucleic Acids Res.* **14**: 2829.